

A Novel DTC Scheme of Double-Star Induction Motors Using Three-Level Voltage Source Inverter

¹R. Zaimeddine and ²E.M. Berkouk

¹Department of Electrical Engineering, Signals and Systems Research Laboratory,
 University of M'hamed Bougara, Boumerdes, Algeria

²Laboratoire Commande Des Processus Ecole National Polytechnique, El Harache, Alger

Abstract: The objective of this study is to study a new control structure for sensorless Double-Star Induction Motors (DSIM) dedicated to electrical drives using a three-level Voltage Source Inverter (VSI). The output voltages of the three-level VSI can be represented by four groups: the zero voltage vectors, the small voltage vectors, the middle voltage vectors and the large voltage vectors in (d, q) plane. Then, the amplitude and the rotating velocity of the flux vector can be controlled freely. Both fast torque and optimal switching logic can be obtained. The selection is based on the value of the stator flux and the torque. Both approaches, two level control and three level control, are simulated. The results obtained show superior performances over the FOC one without need to any mechanical sensor.

Key words: Double-star induction motor, direct torque control, sensorsless control, fast torque response, voltage source inverter

INTRODUCTION

The rapid development of the capacity and switching frequency of the power semiconductor devices and the continuous advance of the power electronics technology have made many changes in static power converter systems and industrial motor drive areas. The conventional GTO inverters have limitation of their dc-link voltage and switching frequency. Hence, double-star induction motors provide an attractive solution for high power process. The vector control of induction motor drive has made it possible to be used in applications requiring fast torque control such as traction^[1]. In a perfect field oriented control, the decoupling characteristics of the flux and torque are affected highly by the parameter variation in the machine.

The scheme proposed in this study is also based on direct torque and flux control of induction machines fed by two three-phase VSI using a switching table. In this method, the output voltage is selected and applied sequentially to the machine through a look-up table so that the flux is kept constant and the torque is controlled by the rotating speed of the stator flux. The Direct Torque Control (DTC) is one of the actively researched control scheme which is based on the decoupled control of flux

and torque providing a very quick and robust response with a simple control construction in ac drives^[2,3] Fig. 1. Both approaches, two level control and three level control, are presented. This type of system associated to the DSIM presents particular advantages to naval ship propulsion systems which rely on high power quality, survivable drives.

Three-level inverter topology and the npc voltage source:

Figure 2 shows the schematic diagram of Neutral Point Clamped (NPC) three-level VSI. Each phase of this inverter consists of two clamping diodes, four GTO thyristors and four freewheeling diodes. Table 1 shows the switching states of this inverter.

Since three kinds of switching states exist in each phase, a three level inverter has 27 switching states. A two-level inverter is only capable to produce six non-zero voltage vectors and two zero vectors^[1]. Figure 3 shows the representation of the space voltage vectors of a three-level inverter for all switching states (SVV). According to the magnitude of the voltage vectors, we divide them into four groups: the zero voltage vectors (V_0), the small voltage vectors ($V_1, V_4, V_7, V_{10}, V_{13}, V_{16}$), the middle voltage vectors ($V_3, V_6, V_9, V_{12}, V_{15}, V_{18}$), the large voltage vectors ($V_2, V_5, V_8, V_{11}, V_{14}, V_{17}$).

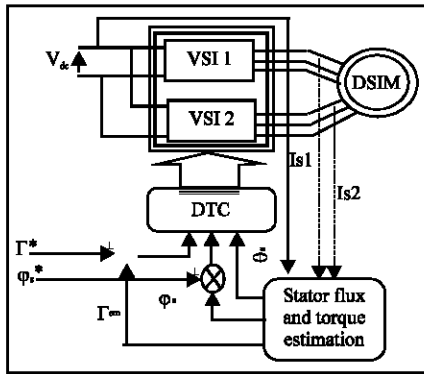


Fig. 1: Block diagram of direct torque control

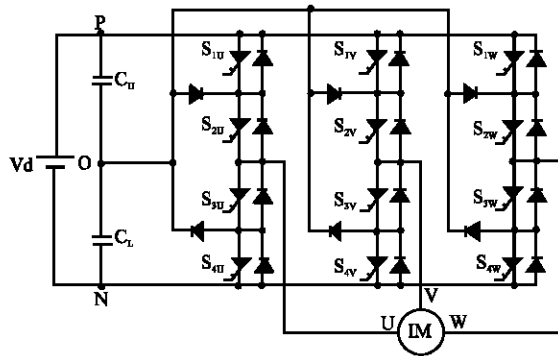


Fig. 2: Schematic diagram of a three-level GTO inverter

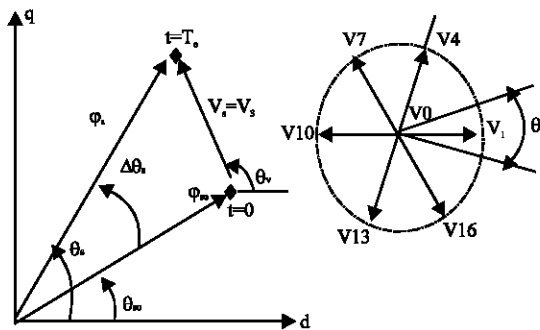


Fig. 3: Flux deviation

Table 1: Switching states of a three-level inverter

Switching states	S ₁	S ₂	S ₃	S ₄	V _N
P	On	On	Off	Off	V _d
O	Off	On	On	Off	V _d /2
N	Off	Off	On	On	0

The Zero Voltage Vector (ZVV) has three switching states, the Small Voltage Vector (SVV) have two and both the Middle Voltage Vector (MVV) and the Large Voltage Vector (LVV) have only one.

Modelling of a double-star induction motor: The double-star induction motor consists of a standard simple

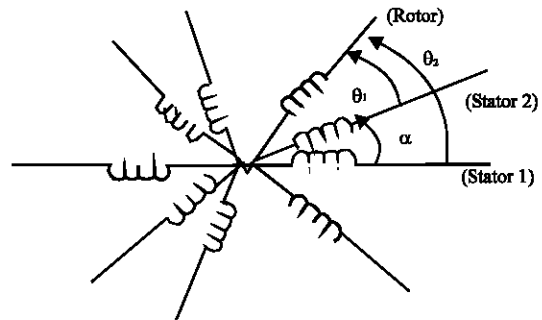


Fig. 4: Windings of the DSIM

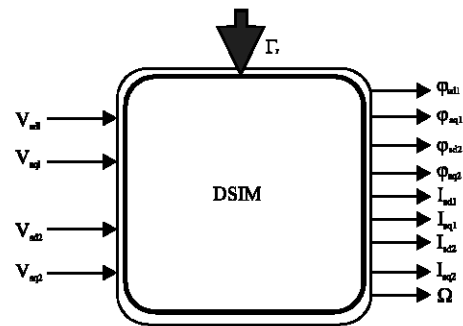


Fig. 5: DSIM model in the stationary reference

squirrel-cage rotor and two separate three-phase stator windings. The windings of the DSIM are shown in Fig. 4.

The following assumptions are made :

- Motor windings are sinusoidally distributed,
- The two star have same parameters,
- Flux path is linear.

Since the two three phase windings wye-connected with isolated neutrals, zero-sequence harmonic currents are non-existent. So, only harmonics of order $3j \pm 1$ ($j=0,1,2,3,\dots$) are considered, by this way a complex model can be derived^[4]. The scheme proposed in this paper is also based on direct torque control of DSIM, while being interested in the angle $\alpha = \pi/6$.

Torque control can be achieved on the basis of its model developed in a two axes (d , q) reference frame stationary with the stator winding, Fig. 5. In this reference frame and with conventional notations (appendix), the electrical mode is described by the following Eq:

$$\frac{d\phi_{sd1}}{dt} = V_{sd1} - R_{s1} i_{sd1} \quad (1)$$

$$\frac{d\phi_{sq1}}{dt} = V_{sq1} - R_{s1} i_{sq1} \quad (2)$$

$$\frac{d\phi_{sd2}}{dt} = V_{sd2} - R_{s2}i_{sd2} \quad (3)$$

$$\frac{d\phi_{sq2}}{dt} = V_{sq2} - R_{s2}i_{sq2} \quad (4)$$

$$\phi_{sd1} = L_{s1} i_{sd1} + L_m (i_{sd1} + i_{sd2} + i_{rd}) \quad (5)$$

$$\phi_{sq1} = L_{s1} i_{sq1} + L_m (i_{sq1} + i_{sq2} + i_{rq}) \quad (6)$$

$$\phi_{sd2} = L_{s2} i_{sd2} + L_m (i_{sd1} + i_{sd2} + i_{rd}) \quad (7)$$

$$\phi_{sq2} = L_{s2} i_{sq2} + L_m (i_{sq1} + i_{sq2} + i_{rq}) \quad (8)$$

$$\phi_{rd} = L_r i_{rd} + L_m (i_{sq1} + i_{sd2} + i_{rd}) \quad (9)$$

$$\phi_{rq} = L_r i_{rq} + L_m (i_{sq1} + i_{sq2} + i_{rq}) \quad (10)$$

$$\Gamma_{em} = P \left[(i_{sq1}\phi_{sd1} - i_{sd1}\phi_{sq1}) + (i_{sq2}\phi_{sd2} - i_{sd2}\phi_{sq2}) \right] \quad (11)$$

$$\phi_s = \sqrt{(\phi_{sd1} + \phi_{sd2})^2 + (\phi_{sq1} + \phi_{sq2})^2} \quad (12)$$

The mechanical mode associated to the rotor motion is described by :

$$J \frac{d\Omega}{dt} = \Gamma_{em} - \Gamma_r(\Omega) \quad (13)$$

$\Gamma_r(\Omega)$ and Γ_{em} are respectively the load torque and the electromagnetic torque developed by the machine.

Stator flux and torque estimation: Basically, DTC schemes require the estimation of the stator flux and torque. The stator flux evaluation can be carried out by different techniques depending on whether the rotor angular speed or (position) is measured or not. For sensorless application, the “voltage model” is usually employed^[5]. The stator flux can be evaluated by integrating from the stator voltage equation.

$$\phi_s(t) = \int (V_s - R_s I_s) dt \quad (14)$$

This method is very simple requiring the knowledge of the stator resistance only. The effect of an error in R_s is usually quite negligible at high excitation frequency but becomes more serious as the frequency approaches zero^[5].

The deviation obtained as the end of the switching period T_e can be approached by the first order Taylor Seri as below.

$$\begin{aligned} \Delta\phi_s &\approx V_s T_e \cos(\theta_v - \theta_s) \\ \Delta\theta_s &\approx T_e \frac{V_s \sin(\theta_v - \theta_s)}{\phi_{so}} \end{aligned} \quad (15)$$

Considering the combination of states of switching functions S_a, S_b, S_c . Fig. 3 shows the adequate voltage vector selection we can increase or decrease the stator flux amplitude and phase to obtain the required performances. The electric torque is estimated from the flux and current information as^[11]:

$$\Gamma_{em1} = P (i_{sq1}\phi_{sd1} - i_{sd1}\phi_{sq1}) \quad (16)$$

APPENDIX

List of the used notations: d, q: indices for (d, q) components; s, r: indices variables; L: magnetizing Inductance; L_m : mutual inductance; V: voltage; i: current; ϕ : flux; R: resistance; Γ_{em} : electromagnetic torque; J: rotor inertia P: number of pairs of poles; ω_s : statoric pulsation; V_{dc} : dc-link voltage; K_f : friction Coefficient; T_e : sampling time; E: error of the variables; ω_r : electric rotor speed; $\Omega = P \omega_r$; ctpl: torque comparator output; cflx: flux comparator output; α : angle between the two stars

Induction motors parameters: Rated power: 4.5 kW; Rated voltage: 220 V; Rated speed: 2840 rpm; Rated frequency: 50 Hz; Rotor resistance R_r : 2.12 Ω ; Stator inductance L_{s1} : 0.011 H; Stator inductance L_{s2} : 0.011 H; Rated current: 6.5 A; Stator resistance R_{s1} : 1.86 Ω ; Stator resistance R_{s2} : 1.86 Ω ; Rotor inductance: 0.274 H; Magnetizing Inductance: 0.3672 H; Number of poles: 1; Rotor inertia: 0.0625 Kg.m²; Friction Coefficient: 0.008 N.m.s/rd; $V_{dc} = 514$ V; $T_e = 100$ μ s.

PRINCIPLE OF DTC CONTROL

Figure 1 shows a block diagram of the DTC scheme. The reference values of flux, ϕ_s^* and torque, Γ_{em}^* , are compared to their actual values and the resultant errors are fed into a two level comparator of flux and torque.

Table 2: Selection strategy for four-quadrant operation

φ_s	↑	Γ_{em}	↑	Γ_{em}	↓
φ_s	↓	V_{K+1}		V_{K-1}	
φ_s	↑	V_{K+2}		V_{K-2}	

The stator flux angle, θ_s , is calculated by:

$$\theta_s = \arctan \frac{\varphi_{sq}}{\varphi_{sd}} \quad (17)$$

And quantified into 6 levels depending on which sector the flux vector falls into. Different switching strategies can be employed to control the torque according to whether the flux has to be reduced or increased. Each strategy affect the drive behavior in terms of torque and current ripple, switching frequency and two or four-quadrant operation capability. Assuming the voltage drop $R_s i_s$ small, the head of the stator flux φ_s moves in the direction of stator voltage V_s at a speed proportional to the magnitude of V_s according to

$$\Delta\varphi_s = V_s T_e \quad (18)$$

The switching configuration is made step by step, in order to maintain the stator flux and torque within limits of two hysteresis bands. Where T_e is the period in which the voltage vector is applied to stator winding. Selecting step by step the voltage vector appropriately, it is then possible to drive φ_s along a prefixed track curve.

Assuming the stator flux vector lying in the k-th sector ($k=1,2,3,4,5,6$) of the (d, q) plane, in the case of two level inverter, to improve the dynamic performance of DTC at low speed and to allow four-quadrant operation, it is necessary to involve the voltage vectors V_{K-1} and V_{K-2} in torque and flux control. In the following, V_{K-1} and V_{K-2} will be denoted backward voltage vectors in contraposition to forward voltage vectors utilised to denote V_{K+1} and V_{K+2} . A simple strategy which makes use of these voltage vectors is shown in Table 2.

For steady operating conditions, Eq. 16 describing the machine torque can be transformed to a sinus function:

$$\Gamma_{elm0} = \Gamma_{max0} \cdot \sin 2\gamma_0 \quad (19)$$

Γ_{max0} and γ_0 are equation, respectively torque and the difference angle between stator and rotor flux vectors.

$$\Gamma_{max0} = p \cdot \frac{1-\sigma}{2 \cdot \sigma \cdot L_s} \cdot \varphi_{s0}^2; \gamma_0 = \theta_{s0} - \theta_{r0} \quad (20)$$

Equations 19 and 20 are established with the assumption that stator flux and rotor closed values in steady state. For disturbed states, the stator flux angle θ_s has in practice a fast dynamic mode as compared to the rotor flux angle θ_r . If these two assumptions are hold the effect of stator vector voltage on the machine torque can be expressed by the first order Taylor expansion as below

$$\Delta\Gamma_{elm} \approx K_\varphi \cdot \Delta\varphi_s + K_\theta \cdot \Delta\theta_s \quad (21)$$

The sensitivity coefficients K_φ et K_θ are defined by:

$$\begin{cases} K_\varphi = \frac{d\Gamma_{elm}}{d\varphi_s} = \frac{2}{\varphi_{s0}} \cdot \Gamma_{elm0} \\ K_\theta = \frac{d\Gamma_{elm}}{d\theta_s} = 2 \cdot \Gamma_{max0} \cdot \cos 2\gamma_0 \end{cases} \quad (22)$$

linking Eq. 17, 23 and 24 leads to:

$$\begin{aligned} \Delta\Gamma_{elm} = & 2 \cdot \frac{V_s \cdot T_e}{\varphi_{s0}} \cdot \Gamma_{elm0} \cdot \cos(\theta_v - \theta_{s0}) \\ & + \frac{2 \cdot V_s \cdot T_e}{\varphi_{s0}} \cdot \sqrt{\Gamma_{max0}^2 - \Gamma_{elm0}^2} \cdot \sin(\theta_v - \theta_{s0}) \end{aligned} \quad (23)$$

This shows the feasibility torque control by a well selected vectors voltage $\overline{V_s}$ [6].

According to this strategy, the stator flux vector is required to rotate in both positive and negative directions. By this, even at very low shaft speed, large negative values of rotor angular frequency can be achieved, which are required when the torque is to be decreased very fast. Furthermore, the selection strategy represented in Table 2 allows good flux control to be obtained even in the low speed range. However, the high dynamic performance which can be obtained utilising voltage vectors having large components tangential to the stator vector locus implies very high switching frequency.

Switching strategy: The switching strategy in the order of the sector θ_s , is illustrate by Table 2. The flux and torque control by vector voltage has in nature a desecrate behavior. In fact, we can easily verify that the same vector could be adequate for a set of value of θ_s . The number of sectors should be as large as possible to have an adequate decision.

The appropriate vector voltage is selected in the order to reduce the number of commutation and the level of steady-state ripple. For flux control, let the variable E_φ ($E_\varphi = \varphi_s^* - \varphi_s$) be located in one of the three regions fixed by the constraints:

$$E_{\varphi} < E_{\varphi \min}, E_{\varphi \min} \leq E_{\varphi} \leq E_{\varphi \max}, E_{\varphi} > E_{\varphi \max}$$

The switable flux level is then bounded by $E_{\varphi \min}$ and $E_{\varphi \max}$. The regions defined for torque location are also noted by:

$$E_T < E_{T \min}, E_{T \min} \leq E_T \leq E_{T \max}, E_T > E_{T \max}$$

And then controlled by an hysteresis comparator^[1]. We apply the principle of the control while estimating the flux and the couple of every stators, what allows us to get an equivalent machine with the made previously assumptions.

PRINCIPLE OF DIRECT TORQUE CONTROL USING A TWO-LEVEL INVERTER

A switching table is used to select the best output voltage depending on the position of the stator flux and desired action on the torque and stator flux. The flux position in the (d, q) plane is quantified in twelve sectors. Alternative tables exist for specific operation mode. The switching table for the case of a two-level inverter, it is easily possible to expand the optimal vector selection to include the larger number of voltage vectors produced by three-level inverter. The appropriate vector voltage is selected in the order to reduce the number of commutation and the level of steady-state ripple.

For flux control, let the variable E_{φ} ($E_{\varphi} = \varphi_s^* - \varphi_s$) be located in one of the three regions fixed by the constraints:

$$E_{\varphi} < E_{\varphi \min}, E_{\varphi \min} \leq E_{\varphi} \leq E_{\varphi \max}, E_{\varphi} > E_{\varphi \max}$$

The switable flux level is then bounded by $E_{\varphi \min}$ and $E_{\varphi \max}$. The flux control is made by two-level hysteresis comparator. Three regions for flux location are noted, flux as in fuzzy control schemes, by $E_{\varphi n}$ (negative), $E_{\varphi z}$ (zero) and $E_{\varphi p}$ (positive).

A high level performance torque control is required. To improve the torque control let of the mismatch E_T ($E_T = \Gamma_{em}^* - \Gamma_e$) to belong to one of the five regions defined by the constraints:

$$E_T < E_{T \min 2}, E_{T \min 2} \leq E_T \leq E_{T \min 1}, E_{T \min 1} \leq E_T \leq E_{T \max 1}, E_{T \max 1} \leq E_T \leq E_{T \max 2} \text{ and } E_{T \max 2} < E_T$$

The five regions defined for torque location are also noted, as in fuzzy control schemes, by E_{Tnl} (negative large), E_{Tns} (negative small), E_{Tz} (zero), E_{Tps} (positive small), E_{Tpl} (positive large). The torque is then controlled by an hysteresis comparator built with two lower bounds and two upper known bounds^[7].

Switching strategy proposed: The switching strategy in the order of the sector θ_s , is illustrate by each tables. The flux and torque control by vector voltage has in nature a desecrate behavior. In fact, we can easily verify that the same vector could be adequate for a set of value of θ_s , the number of sectors should be as large as possible to have an adequate decision.

For this reason, we propose a new approach for direct torque control using a three-level inverter based on twelve regular sectors noted by θ_1 to θ_{12} .

θ_1				θ_2			
$E_r \backslash E_{\varphi}$	P	Z	N	$E_r \backslash E_{\varphi}$	P	Z	N
PL	5	4	8	PL	5	4	8
PS	3	4	6	PS	6	7	9
ZE	0	0	0	ZE	0	0	0
NS	18	0	15	NS	18	0	15
NL	17	13	14	NL	2	16	17

θ_3				θ_4			
$E_r \backslash E_{\varphi}$	P	Z	N	$E_r \backslash E_{\varphi}$	P	Z	N
PL	8	7	11	PL	8	7	11
PS	6	7	9	PS	9	10	12
ZE	0	0	0	ZE	0	0	0
NS	3	0	18	NS	3	0	18
NL	2	16	17	NL	15	1	2

θ_5				θ_6			
$E_r \backslash E_{\varphi}$	P	Z	N	$E_r \backslash E_{\varphi}$	P	Z	N
PL	11	10	14	PL	11	10	14
PS	9	10	12	PS	12	13	15
ZE	0	0	0	ZE	0	0	0
NS	6	0	3	NS	6	0	3
NL	5	1	2	NL	8	4	5

θ_7				θ_8			
$E_r \backslash E_{\varphi}$	P	Z	N	$E_r \backslash E_{\varphi}$	P	Z	N
PL	14	13	17	PL	14	13	17
PS	12	13	15	PS	15	16	18
ZE	0	0	0	ZE	0	0	0
NS	9	0	6	NS	9	0	6
NL	8	4	5	NL	11	7	8

θ_9				θ_{10}			
$E_r \backslash E_{\varphi}$	P	Z	N	$E_r \backslash E_{\varphi}$	P	Z	N
PL	17	16	2	PL	17	16	2
PS	15	16	18	PS	18	1	3
ZE	0	0	0	ZE	0	0	0
NS	12	0	9	NS	12	0	9
NL	11	7	8	NL	14	10	11

θ_{11}				θ_{12}			
$E_r \backslash E_{\varphi}$	P	Z	N	$E_r \backslash E_{\varphi}$	P	Z	N
PL	2	1	5	PL	2	1	5
PS	18	1	3	PS	3	4	6
ZE	0	0	0	ZE	0	0	0
NS	15	0	12	NS	15	0	12
NL	14	10	11	NL	17	13	14

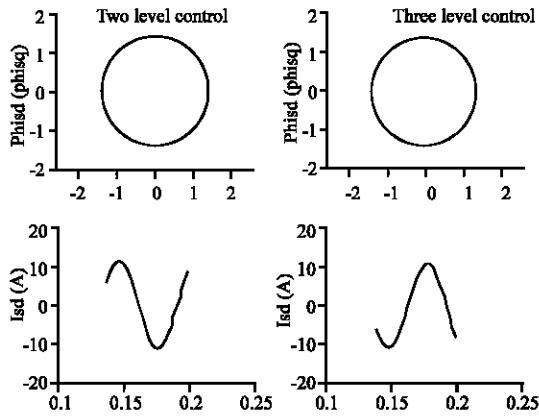


Fig. 6: Vector flux locus and response

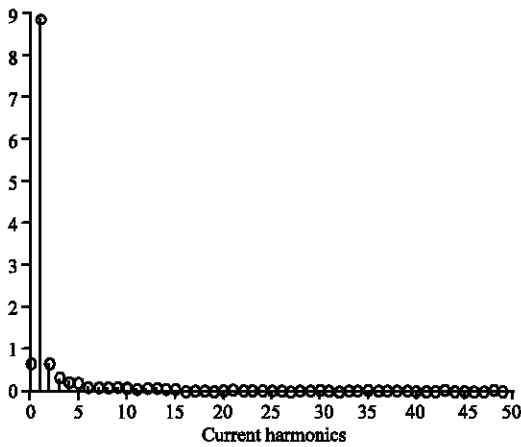


Fig. 7: Current harmonics Isal for three level control

Simulation of the proposed dtc algorithm: The validity and feasibility of the proposed DTC algorithm for three-level voltage source inverter is proved by the simulation results using Matlab-Simulink. The parameters of motors are given in the Appendix. The used flux and torque mismatches for the approach are expressed in percent with respect to the flux and torque reference values.

$$E_{\varphi_{max}} = 2.5\%, E_{\varphi_{min}} = -2.5\%, E_{T_{min}} = -3\%, E_{T_{max}} = 3\%.$$

In the study of a three level-inverter:

$$E_{\varphi_{max}} = 2.5\%, E_{\varphi_{min}} = -2.5\%, E_{T_{min1}} = -0.8\%, E_{T_{min2}} = -3\%, E_{T_{max1}} = 0.8\%, E_{T_{max2}} = 3\%.$$

The simulation results illustrates both the steady state and the transient performance of the proposed torque control scheme. However, the machine has been supposed to run at load.

$$\Gamma_r = \left(\frac{\Gamma_{em}}{\Omega_{ref}} - K_f \right) \cdot \Omega \quad (24)$$

Figure 6 shows the phase current and flux for steady state operation and transient régime at 14 N.m with 1.4 Wb. The wave form of the stator current is closed to a sinusoidal signal. The trajectory of the flux in the case of three level is nearly a circle and answers more quickly compared to the flux response in the case of two level control.

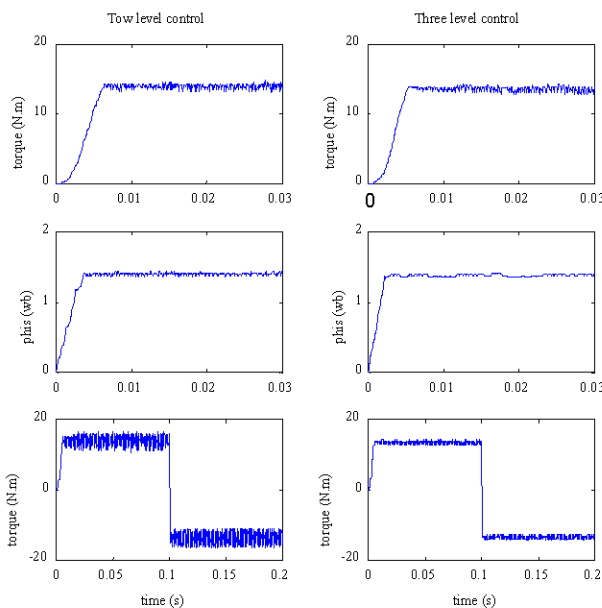


Fig. 8: Torque and flux response

The phase current generated by the three-phase inverter have low harmonic components. Fig.8 shows the current harmonics in the phase I_{sa1} (6 % THD).

Figure 7 shows the torque reverse response from +14 N.m to -14 N.m and flux for 1.4 Wb. The output torque reaches the new reference torque in about 2.5 ms, fast torque response is obtained.

From this analysis high dynamic performance, good stability and precision are achieved.

CONCLUSION

The direct torque control DTC was introduced to give a fast and good dynamic torque and can be considered as an alternative to the field oriented control FOC technique.

High reliability is required, the in-line diagnosis or off-line diagnosis have to be considered in the case of the control using the field-oriented control. A novel DTC scheme of double-star induction motors is proposed in order to develop a suitable dynamic. Compared to classical Field Oriented Control (FOC), which necessitates generally three feedback loops with PI regulators, a current-regulated PWM converter and two coordinate transformations, Direct Torque Control (DTC) uses only a couple of hysteresis comparators to perform both torque and flux dynamic control. The results obtained show superior performances over the FOC one without need to any mechanical sensor.

It is concluded that the proposed control produces better results for transient state operation than the conventional direct torque control. In this study, a DTC systems using a two three-level source inverter is presented it is suitable for high-power applications

REFERENCES

1. Takahashi, I. and T. Noguchi, 1986. A new quick-response and high-efficiency control strategy of an induction motor. *IEEE Trans.*, pp: 820-827.
2. Trounce, J.C., S.D. Round and R.M. Duke, 2001. Comparison by Simulation of Three-level Induction Motor Torque Control Schemes for Electrical Vehicle Applications. *Proc. of international power engineering conference*, pp: 294-299.
3. Xuezh, W.U. and L. Huang, 2001. Direct torque control of three-level inverter using neural networks as switching vector selector. *IEEE IAS, Annual Meeting*.
4. Hadiouche, D., H. Razik and A. Rezzoug, 2000. Modeling of a Double Star-induction Motor with an Arbitrary Shift Angle Between its Three Phase Windings. *Proc. EPE-PEMC'2000, Kosice, Slovak Republic*.
5. Casadei, G. Grandi, G. Serra and A. Tani, 1994. Switching strategies in direct torque control of induction machines., *ICEM*, pp: 204-209.
6. Bacha, A. sbai and R. Dhifau, 1998. Tow Approaches For Direct Torque Control of an Induction Motor. *CESA Symposium on control*, pp: 562-568.
7. Zaimeddine and E.M. Berkouk, 2004. A Novel DTC Scheme for a Three-level Voltage Source Inverter with GTO Thyristors. *SPEEDAM 2004, Symposium on Power Electronics, Electrical Drives, Automation and Motion*, pp: F1A-9-F1A-12.